Steel and Composite Structures, *Vol. 33, No. 2* (*2019*) *181-194*
DOI: https://doi.org/10.12989/scs.2019.33.2.181

A new empirical formula for prediction of the axial compression capacity of CCFT columns

Viet-Linh Tran [1,2a], Duc-Kien Thai [1,2b] and Seung-Eock Kim*[1]

[1] *Department of Civil and Environmental Engineering*, *Sejong University*, *98 Gunja-Dong*, *Gwangjin-Gu*, *Seoul 05006*, *South Korea*
[2] *Department of Civil Engineering*, *Vinh University*, *Vinh 461010*, *Vietnam*

(*Received December 27, 2018, Revised April 20, 2019, Accepted September 30, 2019*)

Abstract. This paper presents an efficient approach to generate a new empirical formula to predict the axial compression capacity (ACC) of circular concrete-filled tube (CCFT) columns using the artificial neural network (ANN). A total of 258 test results extracted from the literature were used to develop the ANN models. The ANN model having the highest correlation coefficient (*R*) and the lowest mean square error (*MSE)* was determined as the best model. Stability analysis, sensitivity analysis, and a parametric study were carried out to estimate the stability of the ANN model and to investigate the main contributing factors on the ACC of CCFT columns. Stability analysis revealed that the ANN model was more stable than several existing formulae. Whereas, the sensitivity analysis and parametric study showed that the outer diameter of the steel tube was the most sensitive parameter. Additionally, using the validated ANN model, a new empirical formula was derived for predicting the ACC of CCFT columns. Obviously, a higher accuracy of the proposed empirical formula was achieved compared to the existing formulae.

Keywords: artificial neural network; axial compression capacity; circular concrete-filled tube; empirical formula

1. Introduction

Steel and concrete are generally combined to form composite members with preeminent characteristics. Owing to the composite action, the composite member is usually stiffer and stronger than the sum of the individual members. Recently, circular concrete-filled tube (CCFT) columns have been widely used in modern construction due to their outstanding structural performance, economic advantages, and aesthetic appeal. A CCFT column provides superior capacities such as high strength, high ductility, and large energy absorption ability. The concrete core in a CCFT column is not only to resist compressive forces but also to prevent the steel member from buckling inward (Bradford *et al*. 2002). Whereas, the steel tube in a CCFT column reinforces the concrete to resist any tensile forces, shear forces, bending moments, and offers confinement to the concrete (Roeder *et al*. 2010).

A large number of experiments has been carried out to investigate the behavior of CCFT columns (Aslani *et al*. 2015, Khan *et al*. 2016, Zhang *et al*. 2016, Nematzadeh *et al*. 2017). Based on the experimental data and mechanical theory, several empirical formulae for predicting the axial compression capacity (ACC) of CCFT columns have been proposed. Some of those were used in design codes such as ACI 318-08 (2011), AISC 360-10 (2010), AS-5100 (2004), and Eurocode-4 (EC-4) (Johnson and Anderson 2004). Although the design codes provide the rule for the design of CCFT columns, some limitations on material strengths and section slenderness still exist, as listed in Table 1. In the past, some authors have modified the existing design formulae based on the miserable extend experimental data or finite element results (Goode and Narayanan 1997, Giakoumelis and Lam 2004, Wang *et al*. 2017). These formulae could provide a better prediction on ACC of CCFT columns, however, they still have some gap between predicting results and many other test results. Hence, a more practical and accurate empirical formula for predicting the ACC of CCFT columns is necessary to cover the wide range of the updating experimental database.

Artificial neural network (ANN) is known as a state-of-the-art approach that imitates the human brain to solve the complex linear and nonlinear relationships in a simple way. ANN operates as a black-box to capture and learn significant structural data (Adeli 2001). Moreover, ANN is often regarded as a superior method for calculating and predicting, compared to classical and traditional methods because of special features, such as low sensitivity to error, massively parallel processing, distributing stored information, its generalization capability, and adaptability to new data. Additionally, the utilization of neural networks is reasonably simple and easy, highly effective, and accurate. Therefore, the ANN approach has rapidly adopted in a variety of fields such as damage detection and identification (Wu *et al*. 1992, Mikami *et al*. 1998, Mohammadhassani *et al*. 2013), optimization (Adeli and Karim 1997, Tashakori and Adeli 2002, Kao and Yeh 2014), prediction (Mukherjee *et al*. 1996, Naderpour *et al*. 2010, Pendharkar *et al*. 2011, Engin *et al*. 2015, Cascardi *et al*. 2017, Karina *et al*. 2017,

*Corresponding author, Ph.D., Professor,
E-mail: sekim@sejong.ac.kr
[a] Ph.D. Student
[b] Ph.D.

ISSN: 1229-9367 (Print), 1598-6233 (Online)

Table 1 Limitations on material strengths and sectional slenderness of the design codes

Standards	Sectional type	D/t	f_y (MPa)	$f_c^{'}$ (MPa)
ACI	Circular	$\leq \sqrt{8E_s/f_y}$	≤ 345	≥ 17.2
AISC		$\leq 0.15E_s/f_y$	≤ 525	$[21 \div 70]$
AS-5100		$\leq 82 \times 250/f_y$	$[230 \div 400]$	$[25 \div 65]$
EC-4		$\leq 900 \times 235/f_y$	$[235 \div 460]$	$[20 \div 60]$

Mandal 2017, Nikbin *et al*. 2017, Tran *et al*. 2019) and given the very promising results.

Nowadays, a large amount of database obtained from the CCFT experiments could be easily achieved in the open literature. A new model that is simple and more accurate than the existing ones can be developed based on the vast experimental database and the advanced technique. Hence, the main objective of this study is to propose a new empirical formula for predicting the ACC of CCFT columns using the modern ANN approach. The accuracy of the proposed formula is compared to the existing formulae.

2. Existing formulae for predicting the ACC of CCFT columns

For the purpose of comparison with the current study, a brief review of some notable existing empirical formulae is presented in this section. Note that the resistance and material partial factors specified in all design codes have been taken as a unity when comparing with the experimental results.

2.1 ACI 318-08 and AS-5100 formulae

According to ACI 318-08 (2011) and AS-5100 (2004), the ACC of CCFT columns is expressed as

$$P_{ACI-AS} = 0.85A_c f_c^{'} + A_s f_y, \tag{1}$$

where A_s and A_c are the cross-sectional area of the steel tube and the concrete core, respectively, f_y is the yield strength of the steel tube, and $f_c^{'}$ is the compressive strength of the concrete core.

2.2 AISC 360-10 formula

The formula for ACC of CCFT columns stated in AISC 360-10 (2010) is expressed as

$$P_{AISC} = P_{no}\left[0.658^{\frac{P_{no}}{P_e}}\right]\frac{P_{no}}{P_e} \leq 2.25$$
$$P_{AISC} = 0.877P_e\frac{P_{no}}{P_e} > 2.25, \tag{2}$$

$$P_{no} = P_p = A_s f_y + 0.95A_c f_c^{'}, \quad \text{for compact section} \tag{2a}$$

$$P_{no} = P_p - \frac{P_p - P_y}{(\lambda_r - \lambda_p)^2}(\lambda - \lambda_p)^2, \quad \text{for non} - \text{compact section} \tag{2b}$$

$$P_y = A_s f_y + 0.7A_c f_c^{'}, \tag{2c}$$

$$\lambda_p = 0.15E_s/f_y, \tag{2d}$$

$$\lambda_r = 0.19E_s/f_y, \tag{2e}$$

$$P_{no} = A_s f_{cr} + 0.7A_c f_c^{'}, \quad \text{for slender section} \tag{2f}$$

$$f_{cr} = \frac{0.72f_y}{\left(\left(\frac{D}{t}\right)\frac{f_y}{E_s}\right)^{0.2}}, \tag{2g}$$

$$P_e = \frac{\pi^2(EI)_e}{L^2}, \tag{2h}$$

$$(EI)_e = E_s I_s + C_3 E_c I_c, \tag{2i}$$

$$E_c = 4700\sqrt{f_c^{'}}, \tag{2j}$$

$$C_3 = 0.6 + 2\left[\frac{A_s}{A_c + A_s}\right] \leq 0.9, \tag{2k}$$

where P_{no} is the nominal compressive capacity of the composite section, P_p is the plastic strength of composite section, P_e is the Euler critical load; P_y is the yield strength of composite section, E_s is the elastic modulus of the steel tube; E_c is the elastic modulus of the concrete core, and f_{cr} is the critical local buckling stress.

2.3 EC-4 formula

According to EC-4 (Johnson and Anderson 2004), the design formula for predicting the ACC of CCFT columns is expressed as

$$P_{EC4} = \eta_a A_s f_y + A_c f_c^{'}\left(1 + \eta_c \frac{t}{D}\frac{f_y}{f_c^{'}}\right), \tag{3}$$

$$\eta_c = 4.9 - 18.5\lambda + 17\lambda^2 \geq 0, \tag{3a}$$

$$\eta_a = 0.25(3 + 2\lambda) \leq 1.0, \tag{3b}$$

$$\lambda = \sqrt{\frac{N_{pl,Rd}}{N_{cr}}} \leq 0.5, \tag{3c}$$

$$N_{pl,Rd} = A_s f_y + A_c f_c^{'}, \tag{3d}$$

$$N_{cr} = \frac{\pi^2(EI)_e}{L^2}, \tag{3e}$$

$$(EI)_e = E_s I_s + 0.6E_c I_c, \tag{3f}$$

where η_a, η_c are the steel reduction factor and the concrete enhancement factor, respectively, λ is the relative slenderness ratio, $N_{pl,Rd}$ is the characteristic plastic cross-sectional compressive resistance, and N_{cr} is the Euler critical load.

2.4 Goode and Narayanan formula

Goode and Narayanan (1997) proposed a formula to predict the ACC of CCFT columns, expressed as

$$P_{GN} = \frac{6t}{(D-2t)} A_c f_y + 0.85 A_c f_c^{'}, \quad (4)$$

where A_c, f_y, and $f_c^{'}$ are the cross-sectional area of the concrete core, the yield and compressive strength of steel tube and the concrete core, respectively, D is the outer diameter of the steel tube, and t is the thickness of the steel tube.

2.5 Giakoumelis and Lam formula

According to Giakoumelis and Lam (2004), the ACC of CCFT columns can be determined using

$$P_{GL} = A_s f_y + 1.3 A_c f_c^{'}, \quad (5)$$

where A_s and A_c are the cross-sectional area of the steel tube and the concrete core, respectively, f_y is the yield strength of the steel tube, and $f_c^{'}$ is the compressive strength of the concrete core.

2.6 Wang et al. formula

Recently, Zhi-Bin Wang *et al*. (Wang *et al*. 2017) used regression analysis of numerical results to conduct a simplified model for predicting the ACC of CCFT columns. The proposed formula is expressed as

$$P_{Wang} = \eta_a A_s f_y + \eta_c A_c f_c^{'}, \quad (6)$$

$$\eta_a = 0.95 - 12.6 f_y^{-0.85} ln(0.14 D/t), \quad (6a)$$

$$\eta_c = 0.99 + [5.04 - 2.37 (D/t)^{0.04} (f_c^{'})^{0.1}] \left(\frac{t f_y}{D f_c^{'}}\right)^{0.51}, \quad (6b)$$

where A_s, A_c, f_y, and $f_c^{'}$ are the cross-sectional area of the steel tube and the concrete core, the yield and compressive strength of the steel tube and the concrete core, respectively, D is the outer diameter of the steel tube, t is the thickness of the steel tube, η_a is a reduction factor (smaller than 1) for the strength contribution of the steel tube to consider the influence of concrete confinement and possible local buckling of the steel tube, and η_c is an amplification factor (larger than 1) to account for the increased strength of concrete due to the confinement effect.

3. Experimental datasets

For the purpose of this study, a total of 258 experimental data were collected from the literature (see Appendix A). These data are taken from the tests conducted by Janss (1974), Lin (1988), Luksha and Nesterovich (1991), O'Shear and Bridge (1994, 1996, 2000), Kato (1995, 1996), Saisho *et al*. (1999), Huang *et al*. (2002), Kang *et al*. (2002), Johansson (2002), Yamamoto *et al*. (2002), Yu *et al*. (2002, 2007), Han and Yao (2003, 2004), Giakoumelis and Lam (2004), Gu *et al*. (2004), Sakino *et al*. (2004), Gardner and Jacobson (1967), Zhang and Wang (2004), Han *et al*. (2005), Tan (2006), Hu *et al*. (2011), Liao *et al*. (2011), Xue *et al*. (2012), Abed *et al*. (2013), Ekmekyapar and Al-Eliwi (2016), Lin *et al*. (2018). In order to ensure the consistency and reliability of the databases, the selection criteria are based on the following: (1) only the circular specimens under monotonic uniaxial compression are included; (2) specimens are not included the internal steel reinforcement, shear stub, tab stiffeners; and (3) to reduce the end effects and minimize the slenderness ratio, the L/D ratio should be from 2 to 4. It is noted that the values of L, D, t, f_y, and $f_c^{'}$ are in the range of 203.20 mm - 3060.70 mm, 89.15 mm - 1020.06 mm, 0.71 mm - 13.26 mm, 181.40 MPa - 853.00 MPa, and 12.00 MPa - 113.49 MPa, respectively. The statistical properties of experimental data are shown in Table 2.

4. Proposed ANN model

4.1 Input and output neurons

The number of input and output neurons are determined by the number of features in the input and output data, respectively. In the current ANN model, L, D, t, f_y, and $f_c^{'}$ were considered as the input parameters, while the axial compression capacity of the CCFT column, P_u was considered as the output parameter.

Table 2 Statistical properties of experimental data

Input data	L (mm)	D (mm)	t (mm)	f_y (MPa)	$f_c^{'}$ (MPa)	P_{exp} (kN)
Minimum	203.20	89.15	0.71	181.40	12.00	435.93
Mean	604.11	196.49	4.06	371.69	53.83	3395.37
Maximum	3060.70	1020.06	13.26	853.00	113.49	45998.17
Standard deviation	394.42	127.30	2.42	126.85	24.34	4887.10
Coefficient of variation	0.65	0.65	0.60	0.34	0.45	1.44

4.2 Learning strategy

Feed-forward back-propagation (BPP) algorithm is widely used in supervised learning technique of ANN (Hornik *et al*. 1989). This is due to its relative simplicity and universal approximation capacity. Supervised learning technique supplies the neural network with inputs and the desired output data. Weights are modified to reduce the difference between the actual and desired outputs. The feed-forward BPP algorithm involves two passes. In the forward pass, the input data are fed to the network at the input layer. Depending on the weights and processing function of each neuron, the input signals propagate along the network to make an output at the output layer. The error between the predicted and actual values is computed. In the backward pass, these error signals are sent back from the output layer to the input layer through the hidden layer. During the BPP of the signals, the weights and bias at each neuron are modified to minimize the output error.

To overcome the over-fitting problem, the Bayesian framework proposed by David MacKay (MacKay 1992) is used. This framework has been implemented in the function "trainbr" of MATLAB software (Beale *et al*. 1992, Bashir and Ashour 2012). Bayesian regularization divides the datasets into two subsets: training and test cases. This algorithm eliminates network weights with small effects on the solution and shows super performance by avoiding local minimums (Jazayeri *et al*. 2016). In this analysis, 258 datasets of the CCFT columns were divided into two parts, in which 220 datasets are used for training (85%) and 38 datasets are used for testing (15%). Owning to the fact that the "trainbr" works best with scaled data, the network inputs and targets are scaled so that they fall in the range of -1 to 1 (Beale *et al*. 1992).

4.3 Activation functions

The activation function is the mechanism by which the artificial neuron processes information and passes it throughout the network. According to Nikbin *et al*. (2017), the activation functions in the hidden and output layers were chosen in the current ANN model as TANSIG and PURELIN, respectively. The TANSIG function transforms values between -1 and +1, meanwhile, the PURELIN function generates the outputs between -∞ and +∞, as shown in Fig. 1.

4.4 Error measurements

The main goal of network training is to optimize the generalization of the network by minimizing network error. In the current ANN model, mean square error (*MSE*) is used to measure the performance of the network, as shown in Eq. (7)

$$MSE = \frac{1}{N}\sum_{i=1}^{N}(e_i)^2 = \frac{1}{N}\sum_{i=1}^{N}(t_i - \alpha_i)^2, \quad (7)$$

where N denotes the number of examples, and t_i, α_i are the target and predicted values of the i^{th} sample.

In order to avoid the over-fitting problem and improve the generalization of the network, the regularization method can be used to modify the error function to be a linear sum of *MSE* and the mean squared network weights and biases, as expressed in Eq. (8)

$$MSEREG = \gamma RMSE + (1-\gamma)MSW, \quad (8)$$

where γ is the performance ratio, $MSW = \frac{1}{n}\sum_{j=1}^{n}\omega_j^2$, is the mean squared weights and biases.

4.5 ANN architecture

There is no reliable rule to determine the number of hidden layers and the number of nodes in the hidden layer. In general, more complex network topologies with a greater number of network connections allow for the learning of more complex problems. However, large neural networks can also be computationally expensive and slow to train. Leung *et al*. (2006), Naderpour *et al*. (2010), and Nikbin *et al*. (2017) showed that the neural network with one hidden layer can obtain the good result compared with experimental data. In the current ANN model, one hidden layer was also adopted and the numbers of neurons in the hidden layers were determined through a trial and error method. The network architecture stands for $mBRn-1$, where m is the number of input node, BR is Bayesian Regularization method, n is the number of hidden nodes and the third digit is the number of output nodes.

Twenty trial networks are carried out in order to find the number of nodes in the hidden layer of the network. All these networks have the same structure and only the number of nodes in the hidden layer is varied, as shown in Fig. 2.

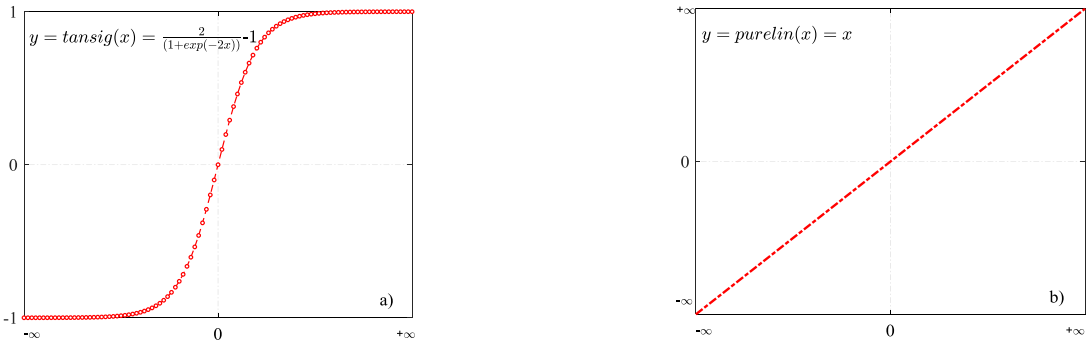

Fig. 1 Activation functions

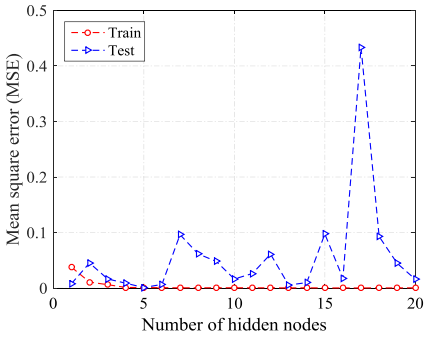

Fig. 2 Maximum mean squared error versus number of hidden-layer neurons

The best ANN model which offered the lowest *MSE* of training and testing was chosen. Eventually, the best configuration with one hidden layer and 5 neurons in the hidden layer was observed, as shown in Fig. 3.

In short, the parameters of the chosen ANN model are listed in Table 3. In this table, some of the parameters are described previously, and others are set as default.

4.6 Performance of the 5BR5-1 model

Fig. 4 shows the performance of the chosen ANN model. Fig. 4(a) shows the training and testing processes of the *5BR5-1* model starting at a large value and decreasing to a smaller one. The best training performance is obtained as 0.001041 at the 145th epoch. A minimum value of the *MSE* defines a good ANN model. Figs. 4(b)-(d) show the coefficients regression of training, testing, and all data of

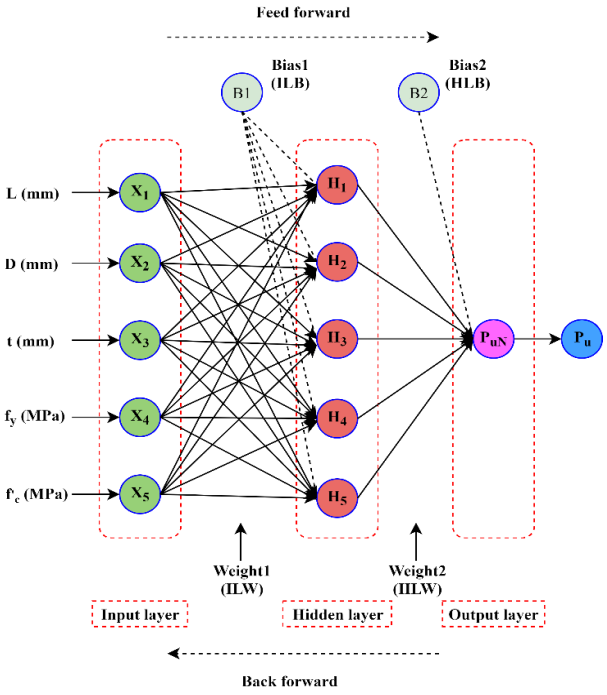

Fig. 3 Schematic architecture of ANN model

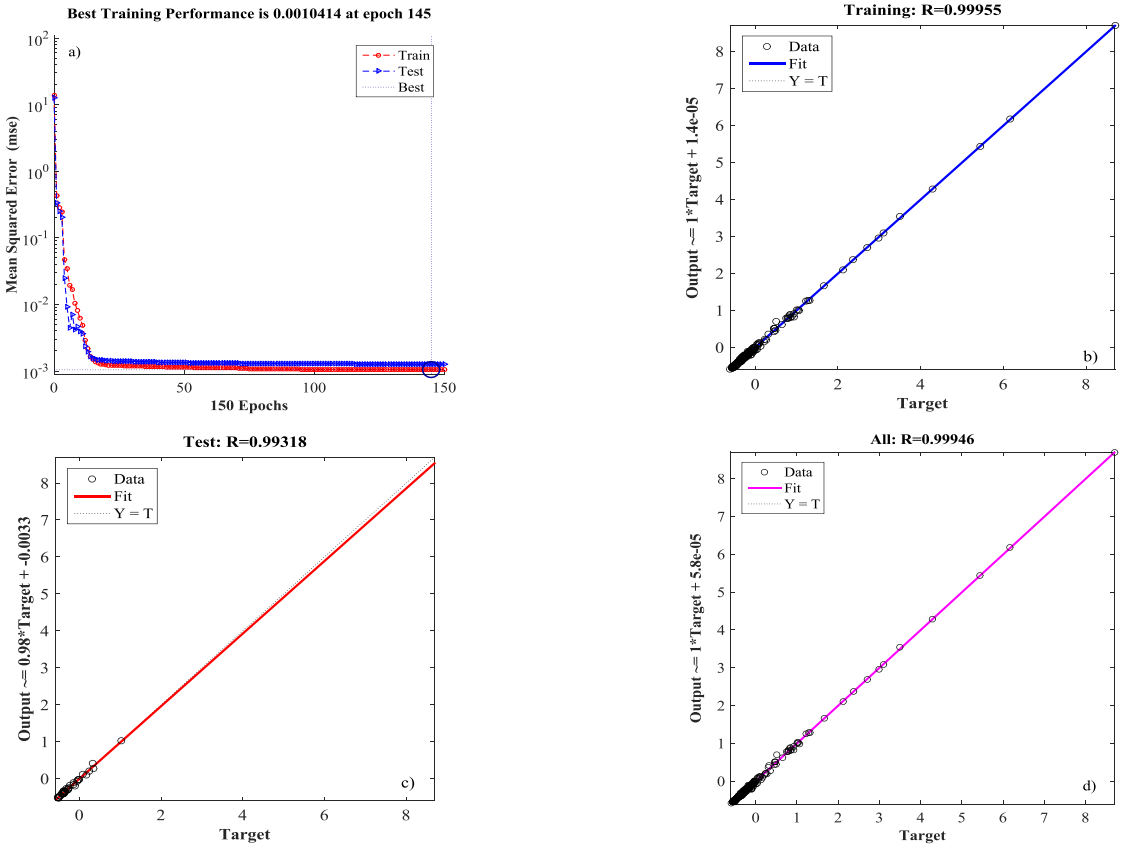

Fig. 4 Performance of the *5BR5-1* model

Table 3 Parameters of the *5BR5-1* model

Description	Value
Training data ratio	0.85
Testing data ratio	0.15
Learning agorithm	TRAINBR
Network type	Feed-forward backprop
Activation functions	TANSIG, PURELIN
Maximum number of epochs to train	150
Performance goal	0
Marquardt adjustment parameter	0.005
Decrease factor for mu	0.1
Increase factor for mu	10
Maximum value for mu	1e10
Generate command-line output	false
Show training GUI	true

the *5BR5-1* model. These figures explain the correlation between the target (experimental data) and the ANN model output. The dashed line in each figure represents the targeted values. The best-fit linear regression line between the outputs and targets is represented by a solid line. The values of the coefficients for training, testing, and all data are found to be 0.99955, 0.99318, and 0.99946, respectively. The overall response with R close to 1 verifying that the training has produced the optimal results.

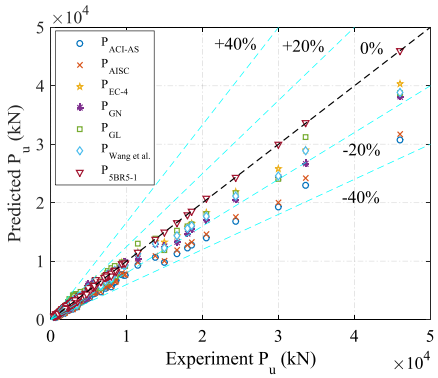

Fig. 5 Comparison between the *5BR5-1* model and existing formulae

5. Comparison of the 5BR5-1 model with the existing formulae

The obtained results from the *5BR5-1* model were compared with the existing formulae to evaluate the capability of the ANN in predicting the ACC of CCFT columns, as illustrated in Fig. 5 and Table 4.

Fig. 5 compares experimental data against predicted data obtained from the *5BR5-1* model and different existing formulae. The more deviation from the dashed line in black color (0% error), the more inaccuracy. As can be seen in this figure, Eqs. (1), (2), (3), (4), (5) and (6) underestimate the ACC of CCFT columns. Meanwhile, Eqs. (3) and (6) have higher accuracy in comparison with Eqs. (1), (2), (4), and (5), however, that is not as accurate as of the *5BR5-1* model.

Table 4 Distribution of error percentages for different models

Error range	Number of data in error range and percentage to total data						
(%)	ACI-AS (Eq. (1))	AISC (Eq. (2))	EC-4 (Eq. (3))	Goode and Narayanan (1997) (Eq. (4))	Giakoumelis and Lam (2004) (Eq. (5))	Wang *et al.* (2017) (Eq. (6))	5BR5-1
± 5	2	6	141	78	73	115	155
	(0.78%)	(2.33%)	(54.65%)	(30.23%)	(28.29%)	(44.57%)	(60.08%)
± 10	11	18	208	160	145	197	226
	(4.26%)	(6.98%)	(80.62%)	(62.02%)	(56.20%)	(76.36%)	(87.60%)
± 15	32	57	247	206	202	244	247
	(12.40%)	(22.09%)	(95.74%)	(79.84%)	(78.29%)	(94.57%)	(95.74%)
± 20	89	136	254	242	229	253	256
	(34.50%)	(52.71%)	(98.45%)	(93.80%)	(88.76%)	(98.06%)	(99.22%)
± 25	176	206	257	256	240	257	256
	(68.22%)	(79.84%)	(99.61%)	(99.22%)	(93.02%)	(99.61%)	(99.22%)
± 30	239	251	258	258	244	258	258
	(92.64%)	(97.29%)	(100%)	(100%)	(94.57%)	(100%)	(100%)
± 35	253	255	258	258	252	258	258
	(98.06%)	(98.84%)	(100%)	(100%)	(97.67%)	(100%)	(100%)
± 40	258	258	258	258	258	258	258
	(100%)	(100%)	(100%)	(100%)	(100%)	(100%)	(100%)

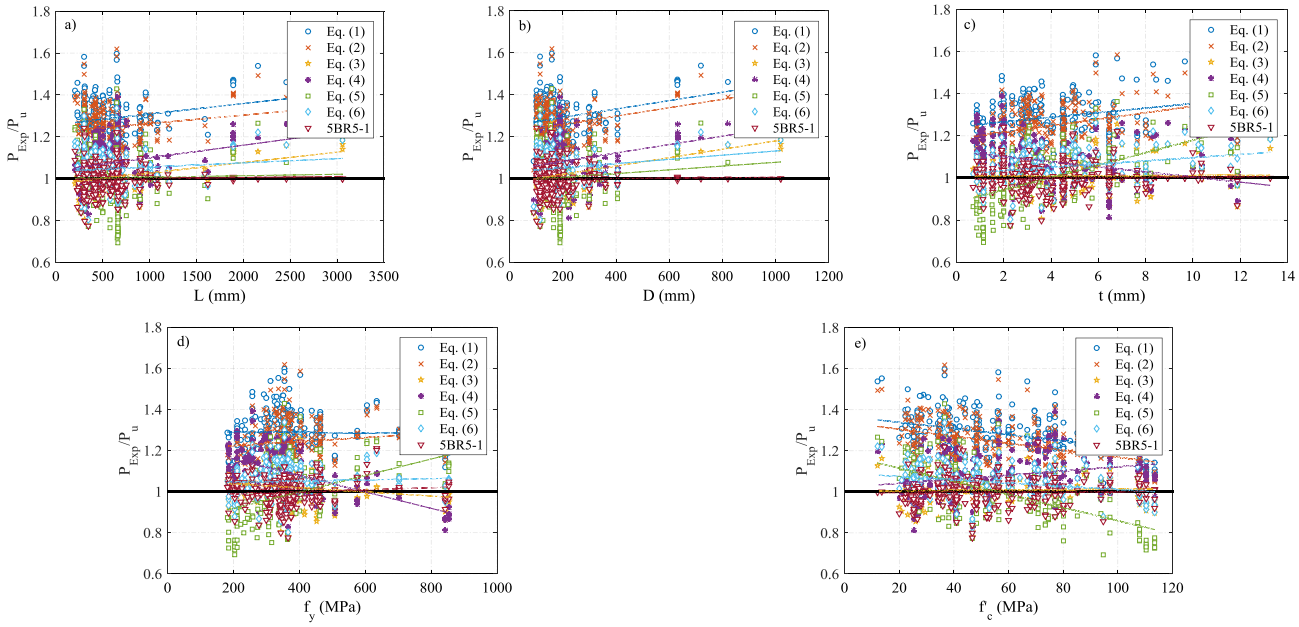

Fig. 6 Stability of different predictions for each input parameter

Table 4 summarizes the error distribution of the *5BR5-1* model and different existing formulae. For the *5BR5-1* model, more than 99% of predicted results are within ± 20% of experimental data, while this value is 52.71%, 34.50%, 98.45%, 93.80%, 88.76%, and 98.06% for Eqs. (1), (2), (3), (4), (5) and (6), respectively. Moreover, 60.08% of the results derived by the *5BR5-1* model, 54.65% of the results derived by Eq. (3), 44.57% of the results derived by Eq. (6), 30.23% of the results derived by Eq. (4), and 28.29% of the results derived by Eq. (5) are within ± 5% of the experimental results whereas Eqs. (1), and (2) reflect poor results in this range of error (±5%). Obviously, the *5BR5-1* model shows excellent performance for predicting the ACC of CCFT columns.

6. Stability analysis, sensitivity analysis, and parametric study

6.1 Stability analysis

Fig. 6 indicates the stability of Eqs. (1), (2), (3), (4), (5), (6) and the *5BR5-1* model in terms of each input parameters. A stable prediction was considered with the ratios of the experimental axial compression capacity (P_u^{exp}) to the predicted one (P_u) close to 1.0 (the solid line in black color) for the entire range of each parameter value. Generally, the existing formulae underestimate the ACC of CCFT columns. Surprisingly, the *5BR5-1* model with the trend line approximately, which lies on the black solid line, is the most stable. This means that the experimental and predicted results are relatively equal.

6.2 Sensitivity analysis

Sensitivity analysis is conducted on the *5BR5-1* model to estimate the influence of input parameters on the ACC of CCFT columns. According to Nikbin *et al.* (2017), each input parameter was divided into five sets including L, ML, M, MH, H, varied from lowest (L) to highest (H) values, in which ML is the midway between L and M, MH is the midway between M and H, as list in Table 5. In the sensitivity analysis, each input parameter varies from its L to H value, while the other parameters are kept constant at their mean values.

Table 5 Quantities regarding each input parameter

Input parameters	L	ML	M	MH	H
L (mm)	203.20	403.65	604.11	1832.40	3060.70
D (mm)	89.15	142.82	196.49	608.27	1020.06
t (mm)	0.71	2.39	4.06	8.66	13.26
f_y (MPa)	181.40	276.54	371.69	612.34	853.00
$f_c^{'}$ (MPa	12.00	32.92	53.83	83.66	113.49

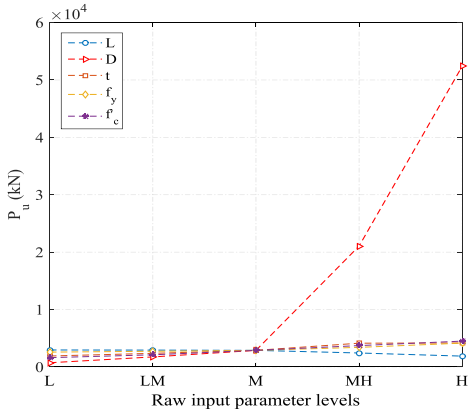

Fig. 7 Sensitivity analysis of input parameters

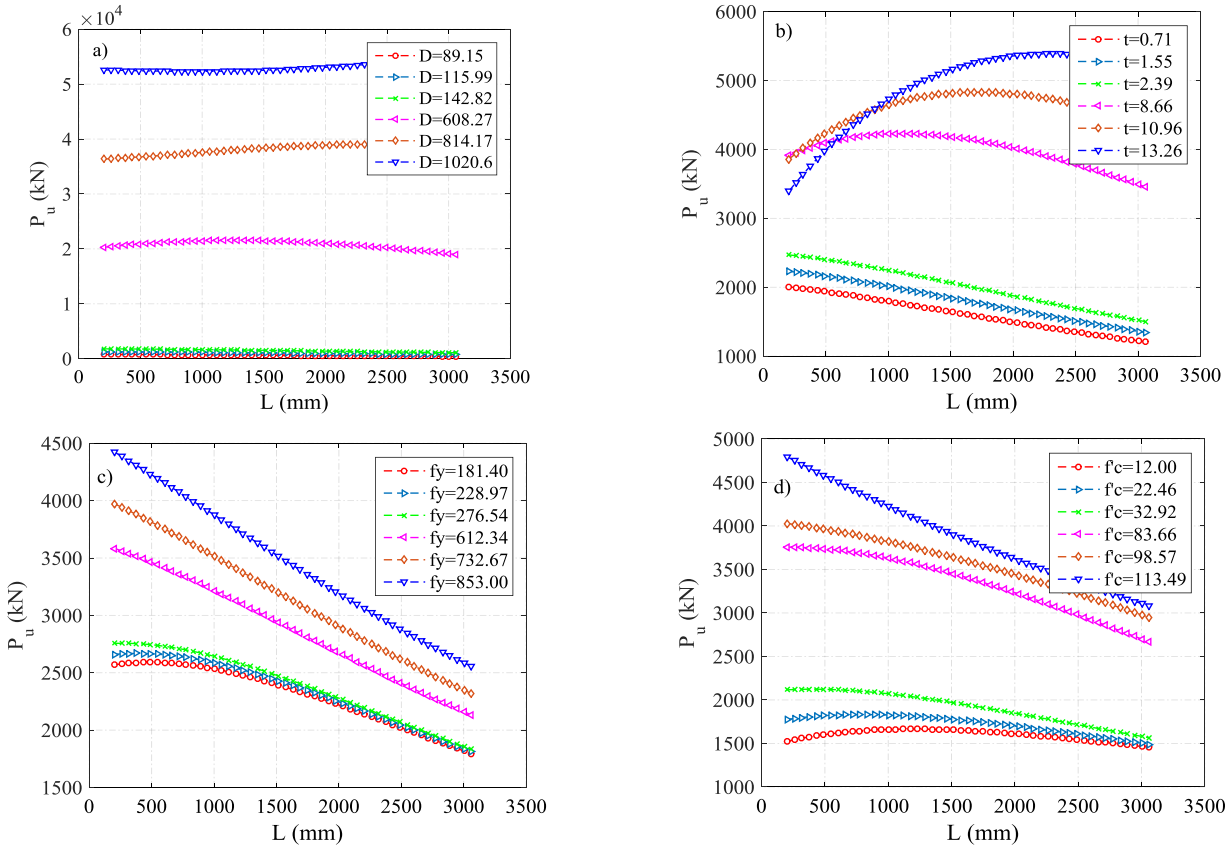

Fig. 8 Effect of the combination of L with parameters D, t, f_y, and $f_c^{'}$ on P_u

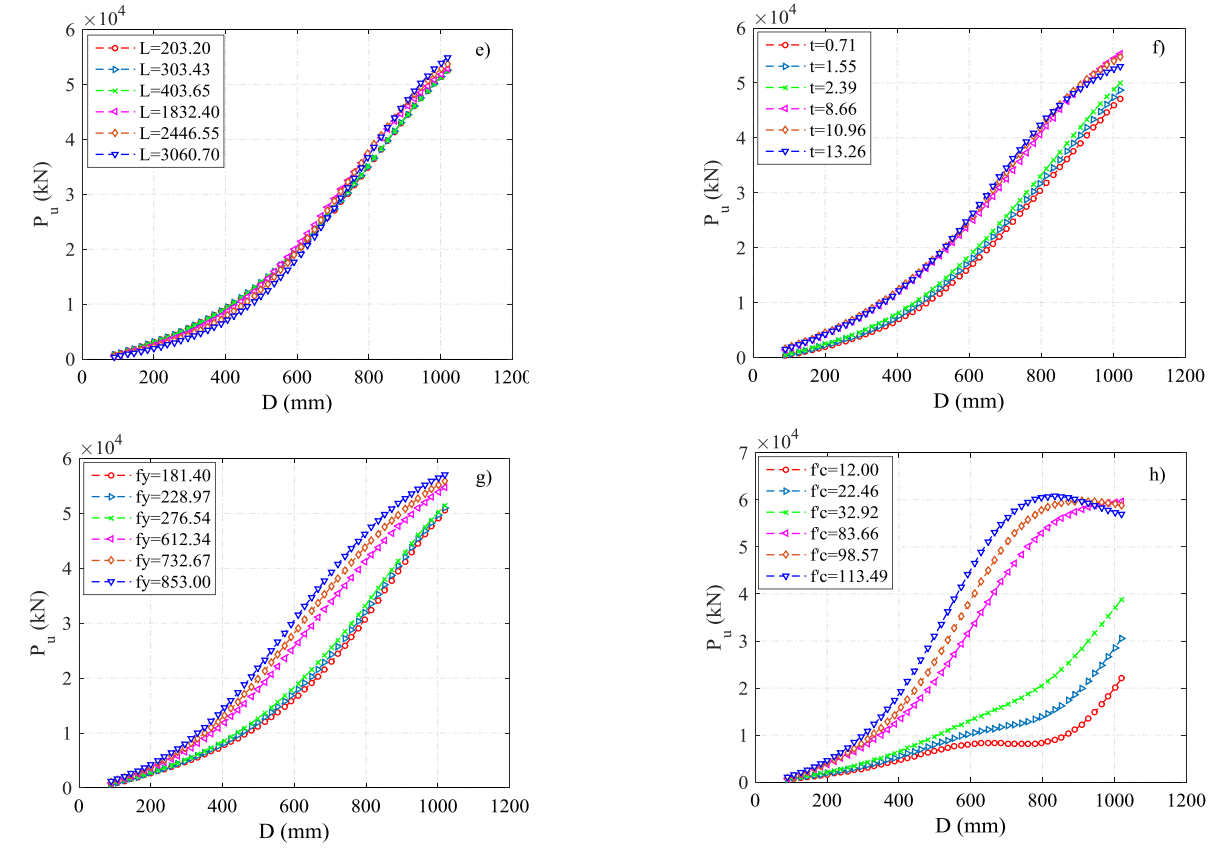

Fig. 9 Effect of the combination of D with parameters L, t, f_y, and $f_c^{'}$ on P_u

Fig. 7 shows the results of sensitivity analysis for different input parameters. As can be seen, all considered parameters govern the axial compression capacity of CCFT columns, however, the outer diameter of the steel tube is the most sensitive one. That means that the outer diameter of the steel tube plays a critical role in predicting the axial compression capacity of the CCFT columns.

6.3 Parametric study

A parametric study is conducted on the *5BR5-1* model to examine the effects of input parameters on the ACC of CCFT columns. In order to investigate the parametric study, an input variable values vary from its minimum to maximum value, while all other parameters are held constant at their mean values. As a result, a total of 120 case studies are simulated, as shown in Figs. 8-12. Fig. 8 shows the effect of the combination of L with parameters D, t, f_y, and$f_c^{'}$ on P_u. It can be seen that the ACC of CCFT columns slightly decreases when the length of the column increases. In contrast, it increases when L is held constant and increasing other parameters.

Figs. 9-12 show the effect of the combination of D with parameters, L, t, f_y, and $f_c^{'}$; the effect of the combination of t with parameters, L, D, f_y, and $f_c^{'}$; the effect of the combination of f_y with parameters, L, D, t, and $f_c^{'}$; and the effect of the combination of $f_c^{'}$ with parameters, L, D, t, and f_y on P_u, respectively.

These figures show that P_u increases when D, t, f_y, and $f_c^{'}$ increase. The effect of the thickness and the yield strength of the steel tube, and the compressive strength of concrete on the ACC of CCFT columns is reasonable. Notably, when the outer diameter of steel tube increases from minimum to maximum value, the ACC of CCFT columns drastically increases.

7. Proposed empirical formula

As seen in the previous sections, the results of the ACC of CCFT column derived from the *5BR5-1* model are in good agreement with the experimental data. However, using the neural network for practical design is not a convenient method. In order to deal with this problem, one practical approach is proposed. Fig. 13 shows the relationship between the most sensitive parameter, D and the ACC of CCFT columns using the *5BR5-1* model. In this figure, the outer diameter of the steel tube varies from minimum to maximum values, while other parameters remain constant at their reference values. Table 6 lists the reference value for each input parameter, these values are chosen to be close to the mean value. According to Leung *et al.* (2006), Naderpour *et al.* (2010), and Nikbin *et al.* (2017), to incorporate the effects of the parameters, L, t, f_y, and $f_c^{'}$ on the formula of the axial compression capacity of CCFT columns, a correction function (F) is derived, as expressed in Eq. (9)

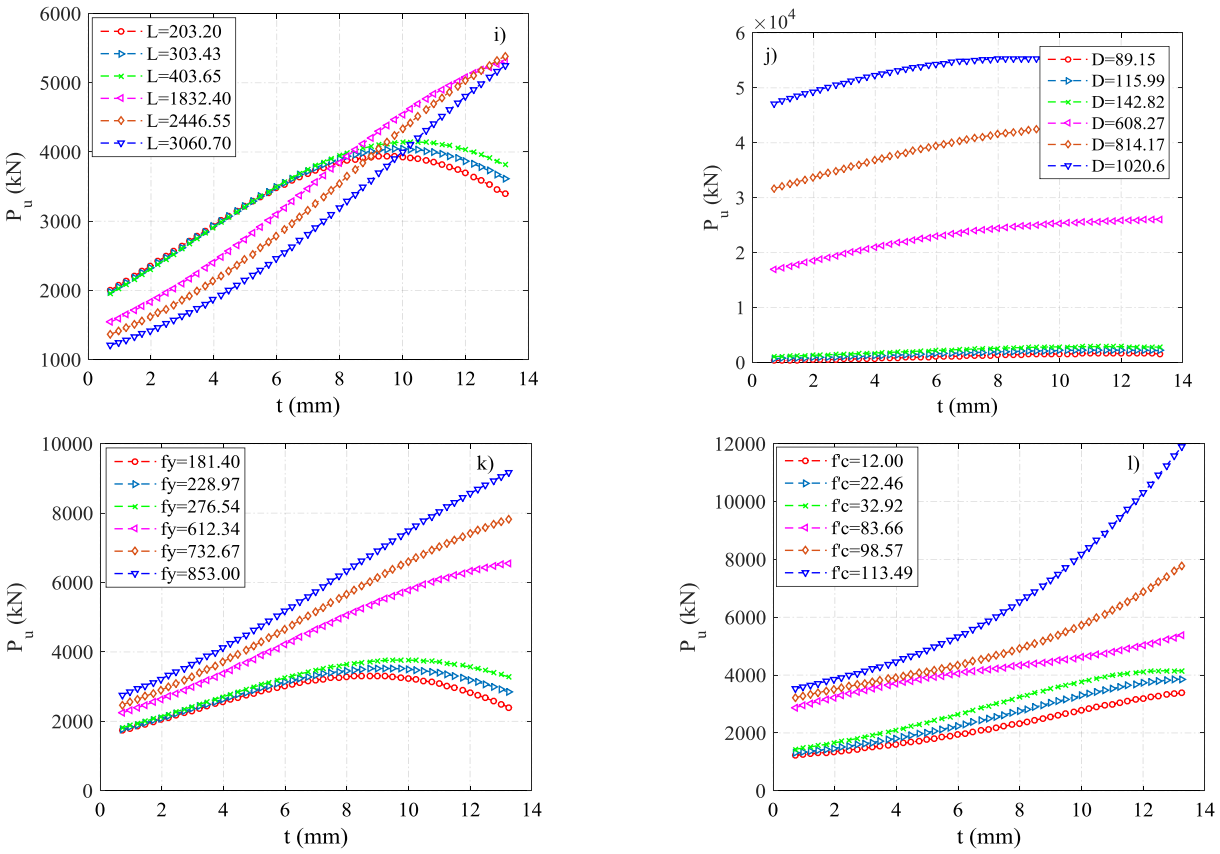

Fig. 10 Effect of the combination of t with parameters L, D, f_y, and $f_c^{'}$ on P_u

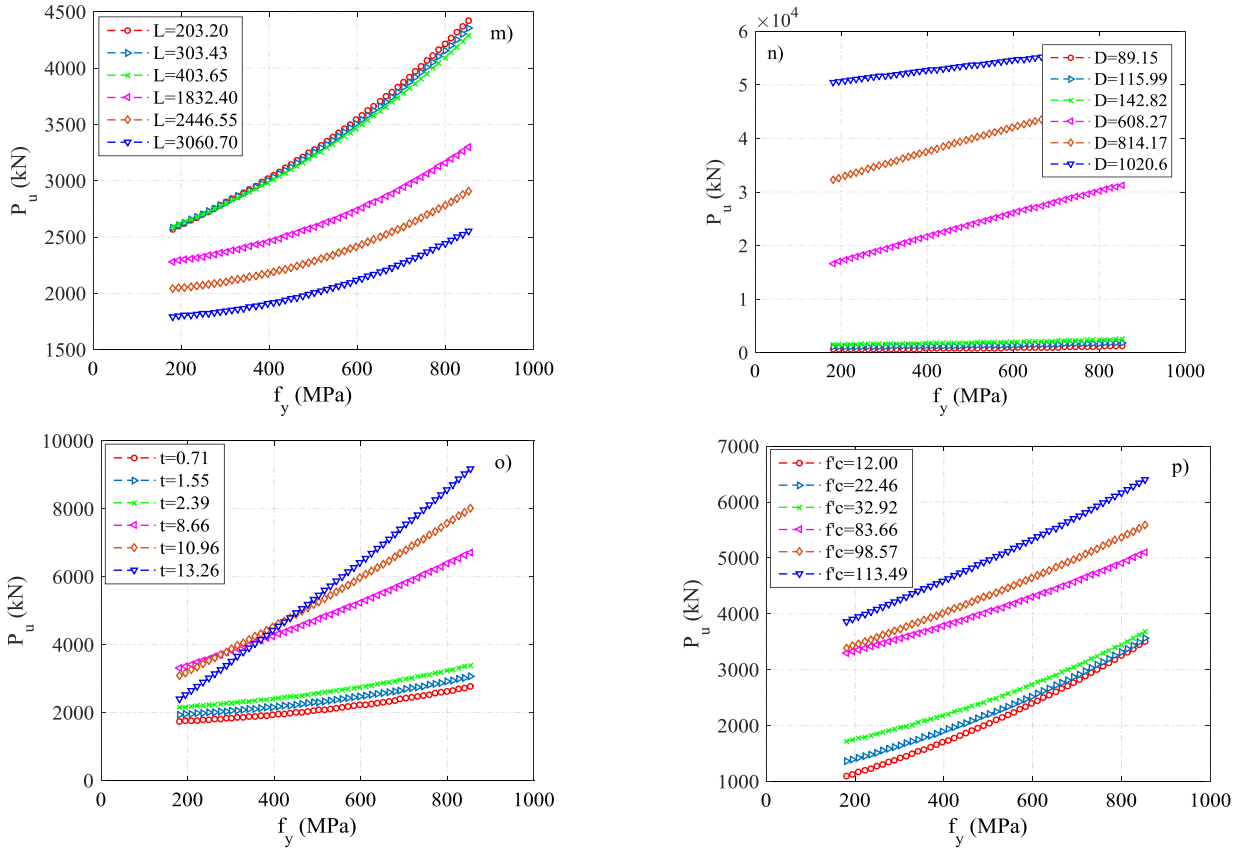

Fig. 11 Effect of the combination of f_y with parameters L, D, t, and $f_c^{'}$ on P_u

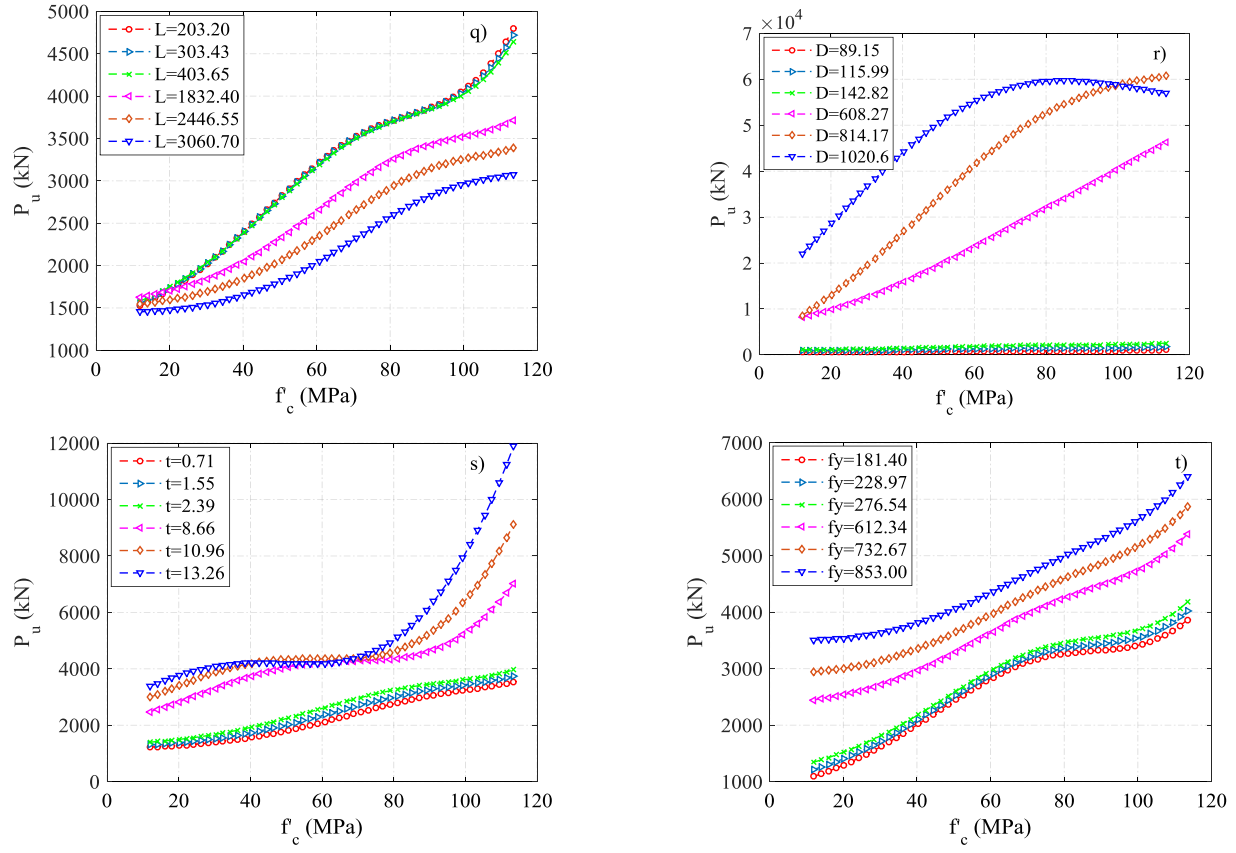

Fig. 12 Effect of the combination of $f_c^{'}$ with parameters L, D, t, and $f_c^{'}$ on P_u

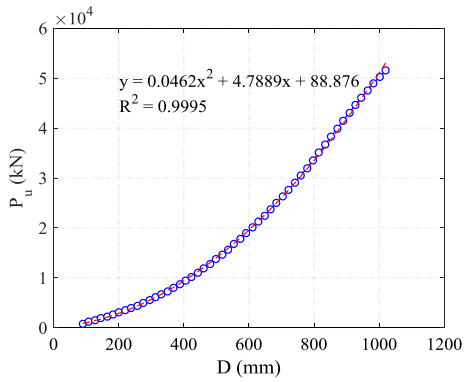

Fig. 13 P_{chart} of ACC at reference parametric values

$$F(L,t,f_y,f_c^{'}) = f_1(L).f_2(t).f_3(f_y).f_4(f_c^{'}) = C_L C_t C_{f_y} C_{f_c^{'}}, \quad (9)$$

In this equation, the variation of P_u with each parameter is supposed to be independent of other parameters. In order to derive the correction factors (C_L, C_t, C_{f_y}, $C_{f_c^{'}}$), a group of curves, called Master Curves, are plotted using the *5BR5-1* model, as shown in Fig. 14.

From this figure, a particular correction factor is plotted against each parameter, while all the other parameters remain constant at their reference values. Ultimately, a fitting curve which has the minimum least square error is chosen to represent as the correction factor for each parameter. For instance, to derive correction factor, C_L, a group of curves are plotted with a variation in $L/600$ (600

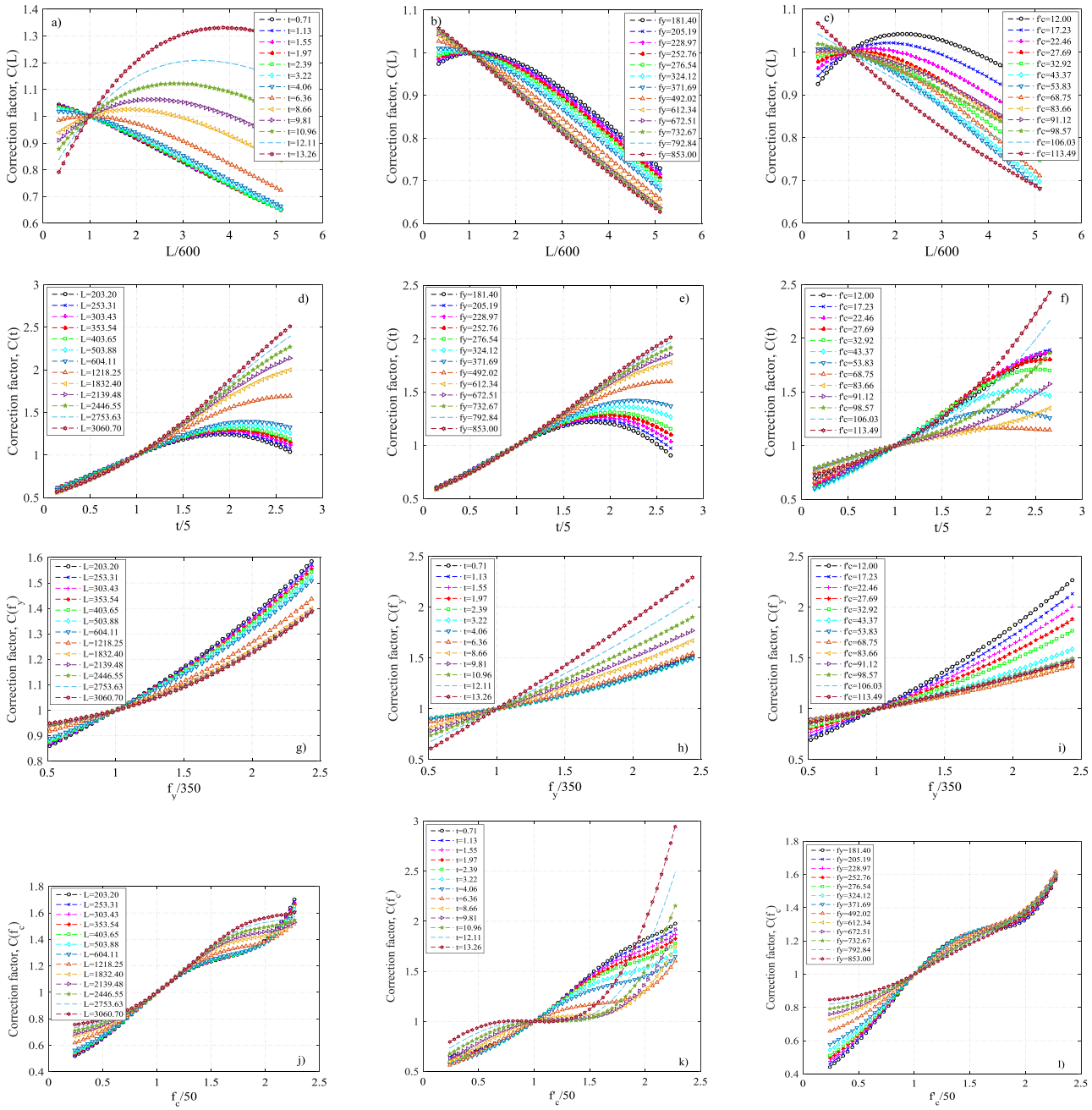

Fig. 14 Correction factors

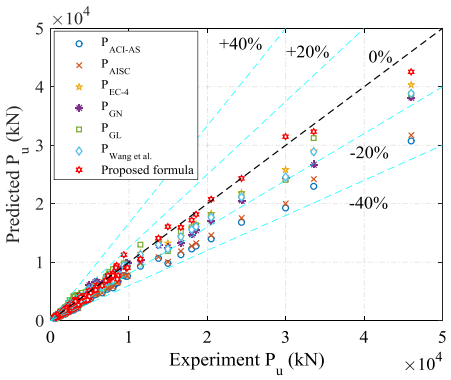

Fig. 15 Comparison between proposed formula and existing formulae

is the reference value of L indicated in Table 6) at different levels of t, f_y, and $f_c^{'}$. Afterward, these curves are divided by the value in which all parameters are fixed in their reference values, as shown in Figs. 14(a)-(c). Finally, a curve in Eq. (10) that has the best fit to the Master Curves of Figs. 14(a)-(c) is established.

$$C_L = 0.0006(\frac{L}{600})^2 - 0.0660(\frac{L}{600}) + 1.0650, \quad (10)$$

In the same manner, the Eqs. (11), (12), and (13) are derived for the correction factor of C_t, C_{f_y}, and $C_{f_c^{'}}$, respectively

$$C_t = -0.0792(\frac{t}{5})^3 + 0.2540(\frac{t}{5})^2 + 0.2770(\frac{t}{5}) + 0.5494, \quad (11)$$

$$C_{f_y} = 0.0701(\frac{f_y}{350})^2 + 0.1114(\frac{f_y}{350}) + 0.8164, \quad (12)$$

$$C_{f_c^{'}} = -0.0539(\frac{f_c^{'}}{50})^3 + 0.1058(\frac{f_c^{'}}{50})^2 + 0.5518(\frac{f_c^{'}}{50}) + 0.3963, \quad (13)$$

Consequently, the axial compression capacity of the CCFT columns (P_u) can be expressed in Eq. (14)

$$P_u = (P_u)_{chart} C_L C_t C_{f_y} C_{f_c^{'}}, \quad (14)$$

Fig. 15 compares the axial compression capacity of the CCFT columns obtained from Eqs. (1), (2), (3), (4), (5), (6), and Eq. (14). Obviously, the ACC of CCFT columns computed by Eq. (14) show reasonable agreement with the experimental data and reflects a superior accuracy. The results obtained from Eq. (14) are based upon a large number of data from the literature, and the equation is reliable to the design of the CCFT column with various parameters lie in the range of the data used for the neural network model. It is concluded that Eq. (14) is simpler and more practical than the ANN model, and it could be considered in practical designs.

8. Conclusions

In this study, the following conclusions can be drawn:

- The ANN approach can be used to predict accurately the axial compression capacity (ACC) of circular concrete-filled tube (CCFT) columns with various geometrical and material properties. In this study, a good agreement between the ANN model and experimental results is achieved.
- Using a reliable *5BR5-1* model, a new formula is derived in order to determine the ACC of CCFT columns. The proposed equation covers a wide range of parameters and shows superior accuracy compared to existing empirical equations.
- The proposed empirical formula show more practical, accurate, and stable than different existing empirical formulae. Hence, it is introduced for the practical design of the CCFT columns.

Acknowledgments

This work was supported by the National Research Foundation of Korea (NRF) grant funded by the Korean government (MSIT) (No. 2019R1A4A1021702).

References

Abed, F., AlHamaydeh, M. and Abdalla, S. (2013), "Experimental and numerical investigations of the compressive behavior of concrete filled steel tubes (CFSTs)", *J. Constr. Steel Res.*, **80**, 429-439. https://doi.org/10.1016/j.jcsr.2012.10.005

ACI 318-08 (2011), Building Code Requirements for Structural Concrete and Commentary (ACI 318-08).

Adeli, H. (2001), "Neural networks in civil engineering: 1989–2000", *Comput.-Aided Civil Infra. Eng.*, **16**(2), 126-142. https://doi.org/10.1111/0885-9507.00219

Adeli, H. and Karim, A. (1997), "Neural network model for optimization of cold-formed steel beams", *J. Struct. Eng.*, **123**(11), 1535-1543. https://doi.org/10.1061/(ASCE)0733-9445(1997)123:11(1535)

AISC Committee (2010), Specification for structural steel buildings (ANSI/AISC 360-10), American Institute of Steel Construction, Chicago, IL, USA.

AS 5100.6 (2004), Bridge design Part 6: Steel and composite construction, AS 5100.6.

Aslani, F., Uy, B., Tao, Z. and Mashiri, F. (2015), "Predicting the axial load capacity of high-strength concrete filled steel tubular columns", *Steel Compos. Struct., Int. J.*, **19**(4), 967-993. https://doi.org/10.12989/scs.2015.19.4.967

Bashir, R. and Ashour, A. (2012), "Neural network modelling for shear strength of concrete members reinforced with FRP bars", *Compos. Part B: Eng.*, **43**(8), 3198-3207. https://doi.org/10.1016/j.compositesb.2012.04.011

Beale, M.H., Hagan, M.T. and Demuth, H.B. (1992), *Neural Network Toolbox™ User's Guide*, The Mathworks Inc.

Bradford, M., Loh, H. and Uy, B. (2002), "Slenderness limits for filled circular steel tubes", *J. Constr. Steel Res.*, **58**(2), 243-252. https://doi.org/10.1016/S0143-974X(01)00043-8

Cascardi, A., Micelli, F. and Aiello, M.A. (2017), "An Artificial Neural Networks model for the prediction of the compressive strength of FRP-confined concrete circular columns", *Eng.*

Struct., **140**, 199-208. https://doi.org/10.1016/j.engstruct.2017.02.047

Ekmekyapar, T. and Al-Eliwi, B.J. (2016), "Experimental behaviour of circular concrete filled steel tube columns and design specifications", *Thin-Wall. Struct*., **105**, 220-230. https://doi.org/10.1016/j.tws.2016.04.004

Engin, S., Ozturk, O. and Okay, F. (2015), "Estimation of ultimate torque capacity of the SFRC Beams Using ANN", *Struct. Eng. Mech*., *Int*. *J*., **53**(5), 939-956. https://doi.org/10.12989/sem.2015.53.5.939

Gardner, N.J. and Jacobson, E.R. (1967), "Structural behavior of concrete filled steel tubes", *J. Proceedings*, **64**(7), 404-413.

Giakoumelis, G. and Lam, D. (2004), "Axial capacity of circular concrete-filled tube columns", *J. Constr. Steel Res*., **60**(7), 1049-1068. https://doi.org/10.1016/j.jcsr.2003.10.001

Goode, C. and Narayanan, R. (1997), "Design of concrete filled steel tubes to EC4", *ASCCS Seminar on Concrete Filled Steel Tubes—A Comparison of International Codes and Practice*.

Gu, W., Guan, C., Zhao, Y. and Cao, H. (2004), "Experimental study on concentrically-compressed circular concrete filled CFRP-steel composite tubular short columns", *J. Shenyang Architect. Civil Eng. Univ. (Natural Science)*, **20**(2), 118-120.

Han, L.-H. and Yao, G.-H. (2003), "Behaviour of concrete-filled hollow structural steel (HSS) columns with pre-load on the steel tubes", *J. Constr. Steel Res*., **59**(12), 1455-1475. https://doi.org/10.1016/S0143-974X(03)00102-0

Han, L.-H. and Yao, G.-H. (2004), "Experimental behaviour of thin-walled hollow structural steel (HSS) columns filled with self-consolidating concrete (SCC)", *Thin-Wall. Struct*., **42**(9), 1357-1377. https://doi.org/10.1016/j.tws.2004.03.016

Han, L.-H., Yao, G.-H. and Zhao, X.-L. (2005), "Tests and calculations for hollow structural steel (HSS) stub columns filled with self-consolidating concrete (SCC)", *J. Constr. Steel Res*., **61**(9), 1241-1269. https://doi.org/10.1016/j.jcsr.2005.01.004

Hornik, K., Stinchcombe, M. and White, H. (1989), "Multilayer feedforward networks are universal approximators", *Neural Networks*, **2**(5), 359-366. https://doi.org/10.1016/0893-6080(89)90020-8

Hu, Y., Yu, T. and Teng, J. (2011), "FRP-confined circular concrete-filled thin steel tubes under axial compression", *J.of Compos. Constr*., **15**(5), 850-860. https://doi.org/10.1061/(ASCE)CC.1943-5614.0000217

Huang, C., Yeh, Y.-K., Liu, G.-Y., Hu, H.-T., Tsai, K., Weng, Y., Wang, S. and Wu, M.-H. (2002), "Axial load behavior of stiffened concrete-filled steel columns", *J. Struct. Eng*., **128**(9), 1222-1230. https://doi.org/10.1061/(ASCE)0733-9445(2002)128:9(1222)

Janss, J. (1974), *Charges ultimes des profils creux remplis de béton chargés axialement*, Centre de Recherches Scientifiques et Techniques de l'Industrie des Fabrications Métalliques

Jazayeri, K., Jazayeri, M. and Uysal, S. (2016), "Comparative analysis of Levenberg-Marquardt and Bayesian regularization backpropagation algorithms in photovoltaic power estimation using artificial neural network", *Industrial Conference on Data Mining*. https://doi.org/10.1007/978-3-319-41561-1_7

Johansson, M. (2002), "The efficiency of passive confinement in CFT columns", *Steel Compos. Struct*., *Int. J*., **2**(5), 379-396. https://doi.org/10.12989/scs.2002.2.5.379

Johnson, R.P. and Anderson, D. (2004), *Designers' Guide to EN 1994-1-1: Eurocode 4: Design of Composite Steel and Concrete Structures. General Rules and Rules for Buildings*, Thomas Telford.

Kang, H., Lim, S. and Moon, T. (2002), "Behavior of CFT stub columns filled with PCC on concentrically compressive load", *J. Architect. Inst. Korea*, **18**(9), 21-28.

Kao, C.-S. and Yeh, I. (2014), "Optimal design of plane frame structures using artificial neural networks and ratio variables", *Struct. Eng. Mech*., *Int. J*., **52**(4), 739-753. https://doi.org/10.12989/sem.2014.52.4.739

Karina, C.N., Chun, P.-j. and Okubo, K. (2017), "Tensile strength prediction of corroded steel plates by using machine learning approach", *Steel Compos. Struct*., *Int. J*., **24**(5), 635-641. https://doi.org/10.12989/scs.2017.24.5.635

Kato, B. (1995), "Strength and Rotation Capacity of Concrete-Filled Tubular Columns, Part 1", *J. Struct. Constr. Eng. (Transactions of AIJ), AJI*, **468**, 183-191.

Kato, B. (1996), "Column curves of steel-concrete composite members", *J. Constr. Steel Res*., **39**(2), 121-135. https://doi.org/10.1016/S0143-974X(96)00030-2

Khan, Q., Sheikh, M.N. and Hadi, M.N. (2016), "Axial compressive behaviour of circular CFFT: Experimental database and design-oriented model".

Leung, C.K., Ng, M.Y. and Luk, H.C. (2006), "Empirical approach for determining ultimate FRP strain in FRP-strengthened concrete beams", *J. Compos. Constr*., **10**(2), 125-138. https://doi.org/10.1061/(ASCE)1090-0268(2006)10:2(125)

Liao, F.-Y., Han, L.-H. and He, S.-H. (2011), "Behavior of CFST short column and beam with initial concrete imperfection: Experiments", *J. Constr. Steel Res*., **67**(12), 1922-1935. https://doi.org/10.1016/j.jcsr.2011.06.009

Lin, C. (1988), "Axial capacity of concrete infilled cold-formed steel columns".

Lin, S., Zhao, Y.-G. and He, L. (2018), "Stress paths of confined concrete in axially loaded circular concrete-filled steel tube stub columns", *Eng. Struct*., **173**, 1019-1028. https://doi.org/10.1016/j.engstruct.2018.06.112

Luksha, L. and Nesterovich, A. (1991), "Strength testing of large-diameter concrete filled steel tubular members", *Proceedings of the Third International Conference on Steel-Concrete Composite Structures, Wakabayashi, M.(ed.), Fukuoka, Japan, Association for International Cooperation and Research in Steel-Concrete Composite Structures*.

MacKay, D.J. (1992), "Bayesian interpolation", *Neural Computat*., **4**(3), 415-447. https://doi.org/10.1162/neco.1992.4.3.415

Mandal, P. (2017), "Artificial neural network prediction of buckling load of thin cylindrical shells under axial compression", *Eng. Struct*., **152**, 843-855. https://doi.org/10.1016/j.engstruct.2017.09.016

Mikami, I., Tanaka, S. and Hiwatashi, T. (1998), "Neural Network System for Reasoning Residual Axial Forces of High-Strength Bolts in Steel Bridges", *Comput.-Aided Civil Infra. Eng*., **13**(4), 237-246. https://doi.org/10.1111/0885-9507.00102

Mohammadhassani, M., Nezamabadi-Pour, H., Suhatril, M. and Shariati, M. (2013), "Identification of a suitable ANN architecture in predicting strain in tie section of concrete deep beams", *Struct. Eng. Mech*., *Int. J*., **46**(6), 853-868. https://doi.org/10.12989/sem.2013.46.6.853

Mukherjee, A., Deshpande, J. and Anmala, J. (1996), "Prediction of buckling load of columns using artificial neural networks", *J. Struct. Eng.*, **122**(11), 1385-1387. https://doi.org/10.1061/(ASCE)0733-9445(1996)122:11(1385)

Naderpour, H., Kheyroddin, A. and Amiri, G.G. (2010), "Prediction of FRP-confined compressive strength of concrete using artificial neural networks", *Compos. Struct*., **92**(12), 2817-2829. https://doi.org/10.1016/j.compstruct.2010.04.008

Nematzadeh, M., Hajirasouliha, I., Haghinejad, A. and Naghipour, M. (2017), "Compressive behaviour of circular steel tube-confined concrete stub columns with active and passive confinement", *Steel Compos. Struct*., *Int. J*., **24**(3), 323-337. https://doi.org/10.12989/scs.2017.24.3.323

Nikbin, I.M., Rahimi, S. and Allahyari, H. (2017), "A new empirical formula for prediction of fracture energy of concrete based on the artificial neural network", *Eng. Fract. Mech*., **186**,

466-482. https://doi.org/10.1016/j.engfracmech.2017.11.010
O'Shea, M.D. and Bridge, R.Q. (1994), "Tests of thin-walled concrete-filled steel tubes".
O'Shea, M.D. and Bridge, R.Q. (1996), "Circular thin-walled tubes with high strength concrete infill", *Composite construction in steel and concrete III*, pp. 780-793.
O'Shea, M.D. and Bridge, R.Q. (2000), "Design of circular thin-walled concrete filled steel tubes", *J. Struct. Eng*., **126**(11), 1295-1303. https://doi.org/10.1061/(ASCE)0733-9445(2000)126:11(1295)
Pendharkar, U., Chaudhary, S. and Nagpal, A. (2011), "Prediction of moments in composite frames considering cracking and time effects using neural network models", *Struct. Eng. Mech*., *Int. J*., **39**(2), 267-285. https://doi.org/10.12989/sem.2011.39.2.267
Roeder, C.W., Lehman, D.E. and Bishop, E. (2010), "Strength and stiffness of circular concrete-filled tubes", *J. Struct. Eng*., **136**(12), 1545-1553. https://doi.org/10.1061/(ASCE)ST.1943-541X.0000263
Saisho, M., Abe, T. and Nakaya, K. (1999), "Ultimate bending strength of high-strength concrete filled steel tube column", *J. Struct. Constr. Eng., AIJ*, **523**(1), 133-140.
Sakino, K., Nakahara, H., Morino, S. and Nishiyama, I. (2004), "Behavior of centrally loaded concrete-filled steel-tube short columns", *J. Struct. Eng*., **130**(2), 180-188. https://doi.org/10.1061/(ASCE)0733-9445(2004)130:2(180)
Tan, K. (2006), "Analysis of formulae for calculating loading bearing capacity of steel tubular high strength concrete", *J. Southwest Univ. Sci. Technol*., **21**(2), 7-10.
Tashakori, A. and Adeli, H. (2002), "Optimum design of cold-formed steel space structures using neural dynamics model", *J. Constr. Steel Res*., **58**(12), 1545-1566. https://doi.org/10.1016/S0143-974X(01)00105-5
Tran, V.-L., Thai, D.-K. and Kim, S.-E. (2019), "Application of ANN in predicting ACC of SCFST column", *Compos. Struct*., 111332. https://doi.org/10.1016/j.compstruct.2019.111332
Wang, Z.-B., Tao, Z., Han, L.-H., Uy, B., Lam, D. and Kang, W.-H. (2017), "Strength, stiffness and ductility of concrete-filled steel columns under axial compression", *Eng. Struct*., **135**, 209-221. https://doi.org/10.1016/j.engstruct.2016.12.049
Wu, X., Ghaboussi, J. and Garrett Jr, J. (1992), "Use of neural networks in detection of structural damage", *Comput. Struct*., **42**(4), 649-659. https://doi.org/10.1016/0045-7949(92)90132-J
Xue, J.-Q., Briseghella, B. and Chen, B.-C. (2012), "Effects of debonding on circular CFST stub columns", *J. Constr. Steel Res*., **69**(1), 64-76. https://doi.org/10.1016/j.jcsr.2011.08.002
Yamamoto, T., Kawaguchi, J. and Morino, S. (2002), "Experimental study of the size effect on the behavior of concrete filled circular steel tube columns under axial compression", *J. Struct. Constr. Eng*., **561**, 237-244.
Yu, Z.-w., Ding, F.-x. and Cai, C. (2007), "Experimental behavior of circular concrete-filled steel tube stub columns", *J. Constr. Steel Res*., **63**(2), 165-174. https://doi.org/10.1016/j.jcsr.2006.03.009
Yu, Z., Ding, F. and Lin, S. (2002), "Researches on Behavior of High-performance Concrete Filied Tubular Steel Short Columns [J]", *J. Build. Struct*., **2**.
Zhang, S.-m. and Wang, Y.-y. (2004), "Failure modes of short columns of high-strength concrete filled steel tubes", *China Civil Eng. J*., **37**(9), 1-10.
Zhang, Y., Fu, G.-Y., Yu, C.-J., Chen, B., Zhao, S.-X. and Li, S.-P. (2016), "Experimental behavior of circular flyash-concrete-filled steel tubular stub columns", *Steel Compos. Struct*., *Int. J*., **22**(4), 821-835. https://doi.org/10.12989/scs.2016.22.4.821